JCBI
Journal of Computing & Biomedical Informatics
ISSN: 2710 - 1606
Volume 08 Issue 01
2024

Research Article
https://doi.org/10.56979/801/2024

Brain Tumor Segmentation and Classification Using ResNet50 and U-Net with TCGA-LGG and TCIA MRI Scans

Muhammad Abdullah Aish[1*], Jawad Ahmad[2], Fawad Nasim[2], Muhammad Javaid Iqbal[2]

[1]Department of Computer Science and Information Technology, The Superior University, Lahore, 54000, Pakistan.
[2]Faculty of Computer Science and Information Technology, The Superior University, Lahore, 54000, Pakistan.
[*]Corresponding Author: Muhammad Abdullah Aish. Email: abdullahaish7@gmail.com

Received: August 09, 2024 **Accepted:** September 25, 2024

Abstract: Brain tumors have become a major source of death in the world. In the case of brain tumor, the brain cells of that particular part grow without any control. The growth has such a serious impact on the normal and healthy cells around the affected part of the brain. Malignancy and benignity are the two types of tumors. Symptoms of the tumor vary according to the place, size, and nature of the tumor. The variable nature of brain tumors is of such a complicated structure that it presents a big challenge for the academics in the field in terms of detection and early classification. A CNN-based model with enhanced "ResNet50 and U-Net architectures" was proposed in this paper. It was used in performing the required analyses on the publicly available "TCGA-LGG and TCIA datasets". The data in the utilized datasets of "TCGA-LGG and TCIA included that of 120 patients". The proposed CNN is used, combined with the fine-tuned ResNet50 model for detecting and classifying tumor versus non-tumor images. The model incorporates the U-Net model to precisely segment the tumor region. Accuracy, Intersection over Union (IOU), Dice Similarity Coefficient (DSC), and Similarity Index (SI) metrics are used for measuring the realization of the model. The quantitative results of fine-tuned "ResNet50 report IOU: 0.91, DSC: 0.95, and SI: 0.95". The combination of U-Net with ResNet50 yielded the best of all, segmenting and classifying tumor regions effectively.

Keywords: Accuracy; Brain Tumor; CNN; Dice Similarity Coefficient; ResNet50; Intersection Over Union; Segmentation; Similarity Index; U-Net

1. Introduction

The human brain comprises various nerve tissues and is characterized by great complexity in its organs. The tissues of the brain regulate almost every vital activity that takes place within the body, including the sensing of the environment, the growth and development of muscles, and the movement of body parts [1]. Every neuron undertakes a range of roles for its own growth and development; however, with time, some of these cells lose their ability to function appropriately, and further with time, they become antagonistic and abnormal in nature. Essentially, "brain tumor refers to the proliferation of abnormal cells in the brain or the central nervous system". The tumors can be of "benign or malignant" nature and might arise in any region of either brain or spinal cord". Genetic mutation, exposure to radiation, and disorders of the immune system are considered some common causes of brain tumors [2, 3].

In addition, even after centuries of advancement in knowledge and biomedical research, malignant proliferation in the brain leading to brain tumors is still one of the biggest problems for humans. The growth rate of this tumor varies from person to person depending on the location and extent of the tumor [4] [5].

Brain tumors are one of the leading causes of death and have the lowest survival rates of all cancers. Brain tumors are difficult to diagnose and identify in the early stages due to their asymmetric shape, texture, location, and distinct borders. The shape of the tumor at its initial point can be accurately determined and then the doctor can decide on the appropriate treatment and save the patient's life [6].

Tumors affecting the brain can be primary or secondary and are often classified as benign or malignant. Noncancerous or benign tumors are slow-growing and do not spread to other parts of the brain. They are often diagnosed and treated later, if still in their early stages. Prostate cancer is cancerous in itself and can be divided into primary and secondary. Brain tumors are tumors that arise from brain cells that are used to grow in the brain. If the cancer starts elsewhere in the body and spreads to the brain, it is called secondary or metastatic (7). Meningiomas, gliomas, and pituitary tumors are some types of brain cancer. The word "meningioma" comes from the three layers of tissue called meninges that surround the brain and spinal cord where the tumor is located. Gliomas are tumors made up of support cells called glial cells that are supported by nerve cells. If the glioma becomes aggressive and directly affects the nervous system, the patient's life expectancy rarely exceeds twenty-four months (8). Another type of unwanted growth can occur in the pituitary gland, which is located at the base of the brain, behind the nose, and controls many other glands in the brain, and can affect many of the body's powers.

One of the most difficult tasks in brain cancer research is to accurately identify the tumor and predict the survival time of the patient after the tumor is diagnosed. Often the information includes images obtained from various methods such as biopsies, spinal samples, CT scans or MRIs. If necessary, the data collected through this process will be subjected to “segmentation, classification and feature extraction”. Deep learning is very good at classification, sorting and certain elimination tasks. However, in brain tumor research, deep learning is often used for classification more than traditional methods such as segmentation, classification and extraction. Traditional machine learning models exist in nature and generally perform well on small amounts of data. This increases the level of abstraction that deep learning currently does, making it more powerful than other methods for prediction and decision making [9].

After the diagnosis of cancer, the accurate classification of brain tumors is a time-consuming process that is necessary for effective treatment planning and follow-up. However, the book's efforts are very laborious and fail to accurately define the area. Therefore, many efforts have been made to develop automatic or semi-automatic segmentation methods for brain tumors [10]. Most of the time, these models are based on design or discrimination. In contrast, the discrimination model uses the features of the image to distinguish between soft tissue and soft tissue. Generative models use the information that will be revealed in the image when segmenting brain tumors. Different classification methods such as SVM and random forest use “images such as histograms of tensor models, image textures, and eigenvalues” to distinguish models [11] [12].

Deep learning is being widely Shannon used for “object identification, classification, and feature extraction”. “Convolutional neural networks are outstanding techniques in semantic image segmentation, and CNN-based algorithms produce reliable results” [13]. They belong to a vast group of advanced mechanisms that are called neural networks and learn directly from the data representations to make any predictions or draw conclusions based on the data. These networks classify and extract features by themselves, both at lower and higher levels. Though CNN-based approaches make effective predictions and conclusions, the major drawback is that they need large volumes of data for training. On the contrary, applying CNN in brain tumor research is tough due to its clinical nature and limited availability of datasets.

In deep learning, such problems can be solved by the transfer learning approach. Basically, it is exploited by two strategies: one is the fine tuning of Convolutional Neural Network, which is specified as ConvONet, whereas the other is freezing its layers. Both the large and small datasets are involved in these transfer learning techniques, which are stated as base and training datasets, respectively. First, a CNN pre-trained on a large dataset is applied to a smaller one. Conventional output is then transformed in general for the small dataset, allowing the model to improve a little more to perform well on the new data. This process may generally be referred to as fine-tuning of the model [14].

MRI-Trauma is a two-dimensional, wide-section, cavity-enhanced MRI image dataset collected from hospitals across China from 2005 to 2020, and is not a tumor.”[15] There is a type of tumor called glioma that occurs in glial cells, the supporting cells found around neurons in the brain. Gliomas can be benign or malignant and can occur in certain areas of the brain or spine. The brain and spinal cord. Although meningiomas are usually slow growing and generally considered benign, they can almost always be malignant [17]. The pituitary gland is classified according to the gland they produce, which is the pituitary

gland located at the base of the central lobe of the brain; Adaptation [18]. Transfer learning is a process where weights from the previous network (learned from large datasets) are applied to small datasets [19].

The present research study introduces a CNN model with fine-tuned ResNet50 architecture for classifying patients with BT and U-Net structure for MRI-based identification. In particular, the research refers to identifying and differentiating patients with tumor and other diseases by applying a "ResNet50 and a U-net-based CNN model". With the help of the confirmation of this paper with the TCGA-LGG and TCIA datasets, the beneficial integration of this computer-aided system is to support the radiologists in decision making regarding the stages of the tumor.

It contributes to the development of a CNN model integrating fine-tuned ResNet50 and U-Net architectures for BT classification and detection from MRI images. By combining the strength of both networks, the network has been driven to produce high accuracy in the said tasks. Detection of BTs would therefore be done by using fine-tuned ResNet50 architecture to classify MRIs as positive or negative for BT. At the same time, the U-Net architecture performs brain tumor segmentation, which involves identifying the tumor itself rather than mixing it up with normal tissues.

By exploiting the strengths of these architectures, this model is able to achieve "high accuracy, precision, recall, and F1 scores" in both detection and segmentation tasks. By doing so, this will go a long way in enhancing speed and accuracy in diagnosing brain tumors to facilitate timely and appropriate treatment decisions that ensure the best possible outcomes for patients.

Next, the remaining parts of the manuscript are organized as: the section Related Work reviewed previous research in this area and the section Methodology described the approach and methods adopted in this work. The section Results shows in some detail the results obtained with the applied models and finally, the section Conclusion synthesizes the findings and discusses some possible future directions.

2. Literature Review

Deng et al. [20] applied CNNs on a "gigantic dataset ImageNet, and achieved the best conclusions in visual recognition tests. Along similar lines", Everingham et al. [21] also reported the best conclusions when CNNs were applied on datasets associated with image classification and detection. In another, using the: Figshare dataset [22]", the adaptive spatial segmentation approach was designed and applied, expanding the tumor regions into the region of interest division and subdivision to get the intensity histograms, grey-level co-occurrence matrix values, and BoW-technique-based features. These achieved accuracy rates of 87.54%, 89.72%, and 91.28%. Mustafa et al. [23] have classified "meningioma, glioma and pituitary tumors with an accuracy of 91%". MRI proposed the use of the 2D Gabor filter for the extraction of statistical features. A multilayer perceptron neural network was used as the classifier for detection, trained through backpropagation. Shakeel et al. [24] used the technique of fractional and multi-fractional dimension to outline the key features. They provided a classification methodology by which the performance for the detection of brain tumors using machine learning and backpropagation may be enhanced.

The researchers in [25] extracted patches from specific regions of candidates by utilizing multiple streams of 2D CNNs, through which lung nodules were identified. Multi-view convolutional networks formed the basis of the architecture for detecting pulmonary nodules. In [26], "tissue segmentation in MRI images was conducted using MATLAB and the ImageJ library", which differentiated between cancerous and non-cancerous tissues. Out of the ten extracted MRI features, certain features were used for brain tumor classification. Various techniques have been applied to create MRI images of the brain. Anil Singh Pirhar [27] proposed a CNN-based approach, where the structure involved tumor classification during preprocessing and post-processing stages, following intensity normalization.

Sultan et al. [28] used two publicly available databases and two different study types to identify tumors including meningiomas, gliomas, and pituitary tumors. One of these criteria is also used to classify gliomas into grades II, III, or IV. The first model achieved 96.13% accuracy, while the second model including 16 CNN layers achieved 98.7% accuracy. Ismail et al. [29] used a small amount of CE-MRI data to classify the same tumors as "meningiomas, gliomas, and pituitary tumors" with 45%, 15%, and 15% accuracy for each tumor type, respectively. Abdullah et al. [30] obtained MRI data from a full brain atlas for their experiments. They preprocessed the dataset and developed a method to distinguish between

tumor and non-tumor images. The system uses an evidence extraction process and provides a computer-aided analysis using an ANN model, which is reported with 99% accuracy and 97.9% sensitivity.

Glioma is the most common type of brain tumor and can be divided into low-grade and high-grade gliomas according to their severity. These groups can also indicate the risk of cancer or breast cancer. In [31], the authors proposed a CNN-based model to classify images of low-grade and high-grade tumors. Finally, the optimized SVM classifier was used to distinguish benign and malignant tumors, including all measurements and results. Lehman et al. [32] used CNN architecture and transfer learning to classify different types of brain diseases. In their transformation study, they adopted ImageNet as the source dataset and Figshare as the target dataset to classify three types of tumors: gliomas, meningiomas, and pituitary tumors. Three CNN models (AlexNet, GoogleNet, and VGGNet) were applied to MRI scans to predict tumor types. To improve the classification, techniques such as transformation learning, smoothing, and freezing are used to enhance pattern recognition in MRI images. Swati et al. [33] proposed a method to standardize T1-weighted contrast-enhanced MRI datasets for brain tumor classification. Compared with traditional machine learning and deep learning CNN, the five-fold validation process achieved an accuracy of 94.82%.

In the context of the glioblastoma brain tumor and the estimation of life expectancy for such patients, Kaoutar et al. [34] outlined the approaches to feature learning and deep learning of MRI images taken from the ImageNet. While working on this dataset, the authors pre-trained a deep CNN, while transfer learning was employed in view of extending the applicability of the pre-trained models to new tasks and at the same time managing the complexity of models that may exhibit when they are subjected to new large datasets. It utilized pre-trained CNN features in survival time prediction and was able to generate results with an "81.8% success rate" after using the flare sequence.

3. Methodology

In this section, the paper explains the method and architecture of the proposal. This tries to present a CNN model that incorporates a fine-tuned ResNet50 coupled with U-Net. Further subsections describe how the model functions and the methodology adopted for the detection and classification of brain tumors.

3.1. Dataset

The dataset used in the present work comprise a sub-sample from "TCGA (The Cancer Genome Atlas) and TCIA (The Cancer Imaging Archive)" [35, 36]. This involved 120 patients with "lower-grade malignant tumors of the nervous system from TCGA". Presence of imaging studies for subjects was possible, and at least one of them was an image with inversion recovery process with regard to fluid attenuation. In view of an informed consent on the existence of genomic constellation information concerning 10 patients, it was possible to exclude these patients and a final sample size of 110 patients was used.

These patients had been divided into 22 non-overlapping clusters of five patients each. The model was cross validated, meaning that one cluster was used as a recognition set while the others are used during training. Imaging Dataset: The dataset consisted of data from The Imaging Archive. Sample images are shown in Figure 1. For this dataset, images corresponding to cases in TCGA were used courtesy of the National Cancer Hospital. If treatment-related imaging data was available, the said ones were used; otherwise, only FLAIR sequences were used. Among these patients, we excluded six patients who did not have both pre-contrast and post-contrast sequences and nine patients with incomplete data of the sequences on the post-contrast study. This then leaves 101 patients who have all the sequences. See Online Resource 1 for more information on the patients. In 20-80 patients, the number of slices was recorded. The bilateral data were reviewed to develop the initial pattern of the growing tumor.

These mutations together with the genomic data of DNA methylation were used in this study. This study has used 6 established pre-existing genetic subtypes of LGG that have been related to distinct tumor features.

3.2. CNN

Convolutional neural networks are currently considered the state-of-the-art for dead group detection in medical imaging [37]. For tumor prediction, only MRI scans will be used in the CNN model without matching faces, which will contain segmentation or labeling information regarding the tumor area. This means that the CNN makes a prediction about the presence of a tumor or other features based on the MRI image itself, without any interference or additional information from the mask.

For a typical CNN, the first layer is the convolutional "Convo" layer, which contains the filters used to convolve the input image to obtain features. The result of this process is usually a set of specifications that show how each filter responds to the input image. Next comes a pooling layer, which usually reduces the size of the feature map but preserves important features. It helps in reducing the number of parameters, which is a way to reduce overfitting. The results of these two layers are flattened and fed to all layers, which provide the final classification based on the results extracted.

The output of the CNN then gives the probability of the class of the book and the threshold for the presence or absence of a tumor can be set. During the training process of the CNN, "backpropagation and stochastic gradient descent" are used to adjust the weights of the training convolutional layers and all layers in order to reduce the number of misclassifications between the required labels and the actual output. After training this CNN, it can detect the occurrence of tumors and classify images as positive tumors if the score is higher than the positive threshold [38].

"The convolutional layer is important in the extraction process and is an important part of the convolutional neural network as shown in Figure 2. The output and size of the layers are calculated by equations (1) and (2) respectively, where FM_b^a is the feature map resulting from the images, Δ is the activation function, I_L is the input width, and K_L^{ief}, Y^{ief} are the filter (f) channels."

$$FM_b^a = \Delta(K_b^a - I_L + Y^i) \quad (1)$$

$$size = \frac{input - filter\ size}{stride} + 1 \quad (2)$$

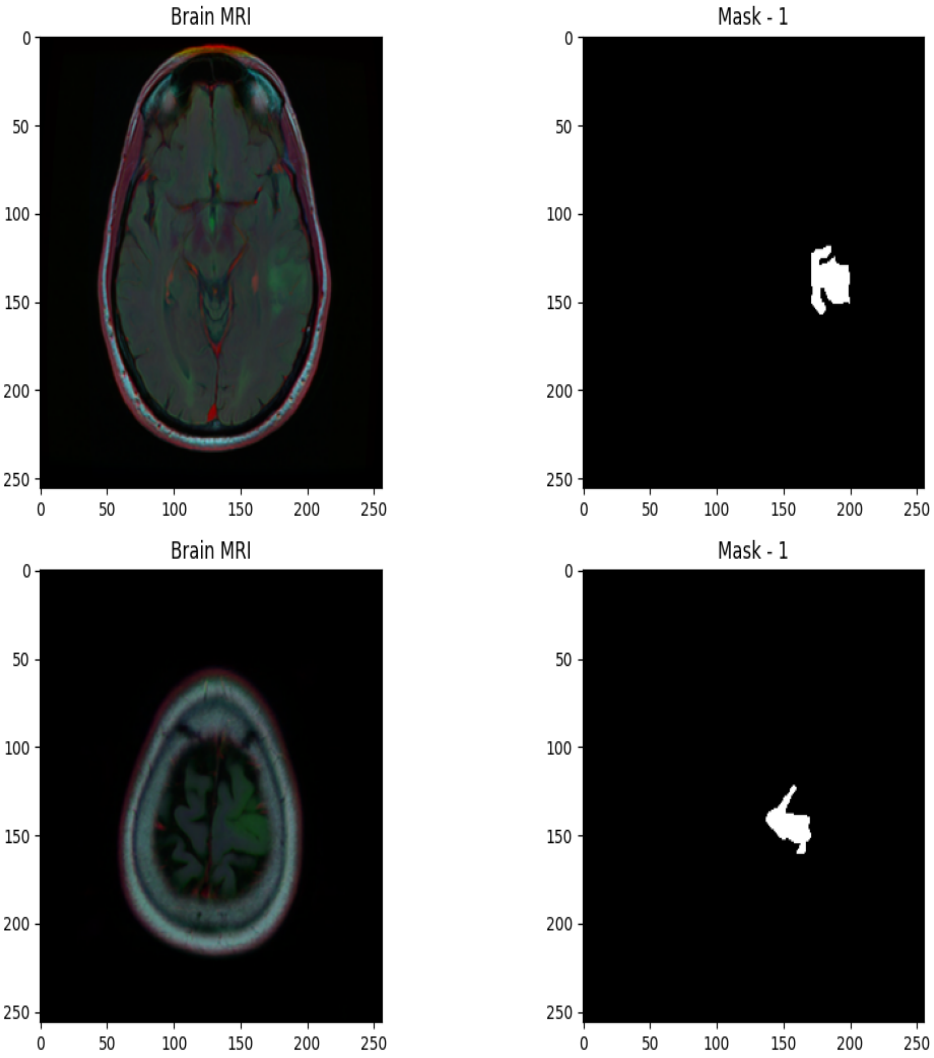

Figure 1. Sample images with their corresponding mask.

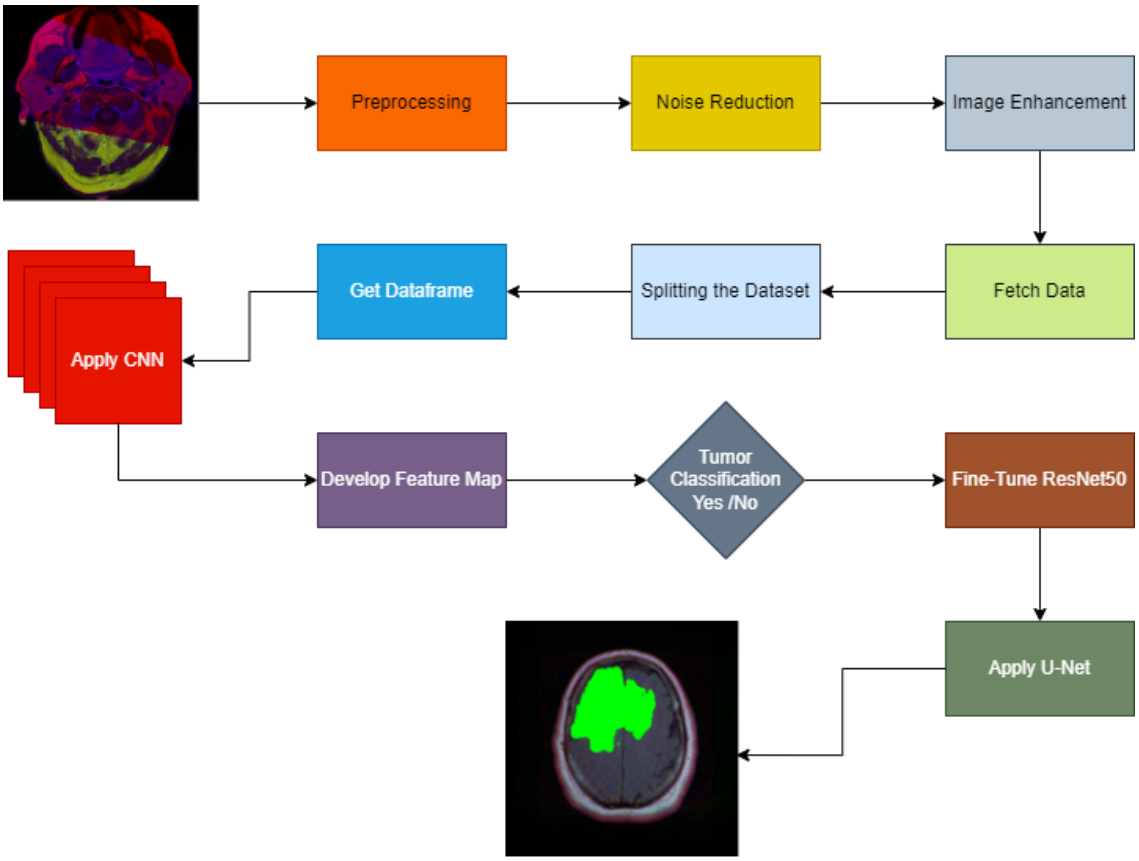

Figure 2. Proposed model architecture.

Pooling layer is an important part of CNN and its two main goals are to reduce overfitting, increase the number of redundant and preserve the original output. Layers that can be used to perform different operations such as max pooling, min pooling and average pooling are the most commonly used ones [39]. This means that the size and output of the pooling layer are determined by equations (3) and (4), where "s" represents the output and "P" represents the area pooling.

$$P_{ij} = max_{p,seR} \quad (3)$$

$$Pooling\ layer\ output\ size = \frac{convo\ output - Pooling\ Size}{stride} \quad (4)$$

The final process is to add three related processes to fine-tune the model. The disadvantage of layer-by-layer tuning is that it is slower because you add one layer at a time. It is used in the same way as a CNN network before training, only a few CNN layers need to be tuned. The CNN layers used to detect brain tumors are shown in the table below: Table 1.

Table 1. Description of CNN Layers.

Layer_Name	Description
Image_Input	Receives the input image, including width, height, and color channels.
Convolutional_Layer	A key component of CNN, responsible for feature extraction from the input data.
Batch Normalization	Normalizes the input by setting the mean to zero and adjusting the variance, which enhances the network's performance.
ReLU (Rectified Linear Unit)	Introduces non-linearity by converting all negative and odd values to zero, while passing positive values unchanged.
Pooling	Manages overfitting and reduces the number of parameters. It follows each convolutional layer and can be applied as min, max, or average pooling.

Softmax	Processes the output from the pooling and convolutional layers, feeding them into the CNN as the initial step for classification.
Fully Connected Layer	Executes the final classification by connecting all the neurons in the network and processing the aggregated input data.
Classification Layer	Calculates the cross-entropy loss for multiclass problems and maps the predicted outputs to the correct class categories.

3.3. ResNet50 Model

The best way to use CNNs for brain tumor detection and MRI image classification is the advantages of ResNet50. Use "ResNet50 CNN pre-training model and ImageNet dataset" to perform various object recognition operations. These include "convolutional layers, pooling layers, and all layers". ResNet50 is used for feature extraction in brain tumor diagnosis. It captures the features of the overall image, which can be useful for detecting brain tumors in low-level processes. Finally, the previous several layers in ResNet50 were replaced with a new set of related methods to detect and classify tumor cells.

The entire model is then fine-tuned on the new MRI scan data by connecting it with the new connected technique. Therefore, the backpropagation of stochastic gradient descent allows the weighting of each layer in the model to be adjusted. The equipment used for classification includes brain MRI scans, and these images are preprocessed to increase the contrast between the tumor and the surrounding healthy tissue before being included in the product. The fine-tuned model shows the probability of classifying the candidate class: tumor (yes) and non-tumor (no). The boundaries of the formation of the urine can then be determined and eventually whether a tumor is present or not.

The ResNet50 model is trained using a CNN in the training phase to extract features from brain MRIs and classify them as tumor or healthy. The features are included in the pre-trained ResNet 50 network for brain diagnosis, and training on new data from MRI scans allows optimization of the application. This is because this method uses MRI data and doctors can predict the detection and distribution of brain tumors with a high degree of accuracy.

3.4. U-Net Model

This design creates applications for deep learning on semantic segmentation problems and is often used for segmentation of brain tumors in MRI images. It is based on two main concepts: contraction method and expansion method. The contraction method uses convolutional and pooling layers to extract high-level abstraction features from MRI images. When the role of the pooling layer is to reduce the spatial dimension of the feature and expand its depth, for example, when the network can capture an abstract representation, the expansion method can include convolutional layers and up sampling layers, so the spatial dimension will increase and the depth of the feature will decrease. There is a combination of compression and expansion layers in the U-Net architecture: this preserves the spatial information that would be discarded due to the down sampling process.

This is called a probability map, and each pixel in the input image is predicted to be a tumor region with a certain value. In general, the probability map can be obtained by using the softmax function in the last layer of the network. During training, we use the backpropagation technique to calculate the weights of the U-Net model, where stochastic gradient descent is often used to optimize the loss function, which should generally be the binary cross entropy. Unemployment (sometimes called rate or target function in other texts) is a measure of the difference between the model's predicted rate and the actual rate of the target variable. It evaluates the performance of the model by the penalty or loss; that is, the larger the difference between the prediction and the actual, the larger the loss.

In fact, unemployment should provide some guidance during the training model. When calculating the loss for the current model used to train the model, the parameters of the model are adjusted to reduce the loss and improve the prediction. This is used as a loss to reduce or increase the weight in the network based on the ground truth segmentation map.

Since the U-Net model is trained, the new segment can be used for other applications in brain tumor MRI. To do this, the input image can be sent to the training model to recover the resulting output map. Therefore, the input data can be sent to the training model to generate the correct output maps.

Probabilistic output can be done after obtaining a binary segmentation map that shows whether each pixel in the input image is a tumor or not. This method has proven to be very useful in these projects and is slowly but steadily becoming one of the methods used in most analyses.

4. Results

A fine-tuning combined method of ResNet50 and U-Net with the convolutional neural network model perhaps works powerfully in comprehensive brain tumor detection, classification, and segmentation. Maximum advantage has been taken from the capabilities of each model in order to enhance the overall accuracy.

4.1. CNN Results

The CNN architecture used also presents relatively good performance for the identification of a brain tumor in this paperwork. Higher results are the "statistical performance, accuracy, precision, recall, the F1 score," and, therefore, this will ensure the model as one of the most welcoming tools for the identification of the brain tumors. It was trained on a labelled tumor and non-tumor brain MRI images dataset. The forecast accuracy of the CNN model was found to be quite high at 92%, more details are depicted from the confusion matrix in figure3. Accuracy and loss over time can be represented graphically as shown in figure 4 where both of them are represented by red and blue curves. Precision, defined as "the ratio of accurately recorded positive detections to the total number of positive detections, was between 90% and 94%". It is worth emphasizing that out of all the actual positive cases, correctly identified positives constituted between 83% and 97%. The support values to "tumor and non-tumor classes" are shown as 219 and 371 in table 2. Likewise, in normal practice "F1 score which is the harmonic mean of precision and recall moved between 0.88% and 0.93%", as shown in Table 2.

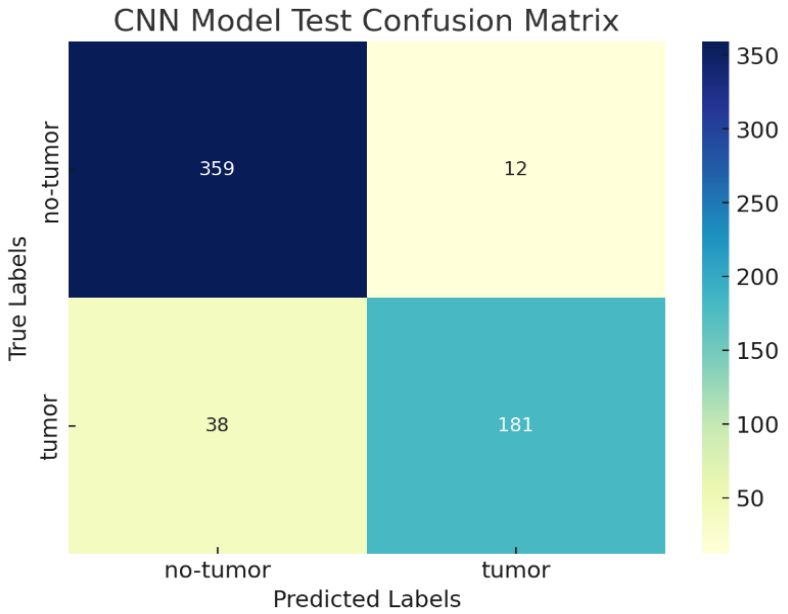

Figure 3. Confusion matrix for CNN model.

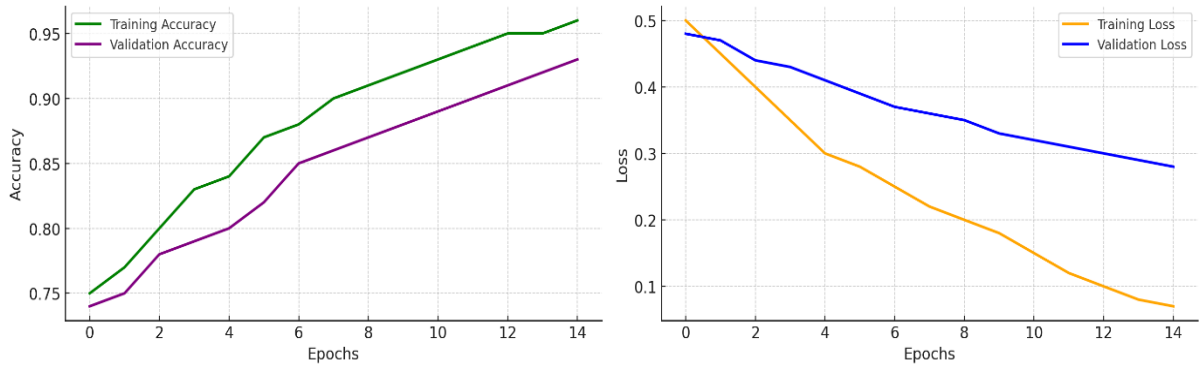

Figure 4. Accuracy and loss graph

Table 2. Model results.

Metrics	Non-Tumor (0)	Tumor (1)
Support	371	219
Accuracy	0.92	0.96
Precision	0.9	0.94
Recall	0.97	0.83
F1-Score	0.93	0.88
DSC	0.95	0.97
IOU	0.91	0.92
SI	0.95	0.97

The CNN model can be thought of as having a high statistical performance, the fact that this justified tool will be useful for radiologists and clinicians; hence, by means of allowing them to detect brain tumors from MRI images with speed and accuracy. This gives an opportunity for clinicians to undertake early treatment owing to early detection, which eventually pays dividends in significantly improving the outcomes of patients.

4.2. ResNet50 Results

It describes a model derived from the CNN architecture known as the fine-tuned ResNet50 model for the classification of brain tumor images. And it was trained a dataset comprises the labelled sets of brain MRI scans for the tumor types and the tumor as well as the non-tumor images. What has been found is that ResNet50 is very effective in the identification of brain tumors, provided an average operation rate of 94% as shown below in the confusion matrix in figure 5. “Accuracy and loss are represented graphically in this context in Figure 6 at the blue and red trend lines respectively. Precision, a measure that determines the percentage of correct classifications of the tumor type amongst all positive classifications, varied within the range of 93% and 96% for this model. Recall, which reflects the true positive rate of the classification of tumor types, is similarly high, varying from 87% to 98%”. In this case, the F1 score was the average of precision and recall, with a harmonic mean. It varies between “0.92% and 0.95%” as presented in the Table 1 below.

Support is 219 in the case of a tumor and 371 for no tumorous cases. “Fine-tuned ResNet50 architecture” in the CNN model proves to be an effective tool for brain tumor classification, achieving ultimate statistical performances. This will support the radiologists and clinicians in the identification of proper types of brain tumors from MRI images for more personalized and effective treatment for patients to bring beneficial results for the patient.

4.3. U-Net Results

Similar criteria can be used to classify brain tumors. The U-Net architecture generates a probability map representing the probability that each pixel in the image falls into the tumor region. Initializing this resulting map will generate a binary segmentation map indicating whether each pixel is a tumor or not. This binary segmentation map can help improve the detection and classification tasks performed by the CNN model when optimizing ResNet50. For example, with the help of segmentation maps, the model can only consider the tumor area, thus increasing the overall accuracy and reducing the negative.

The results from the CNN model using “fine-tuned ResNet50 and U-Net” are combined to evolve a binary segmentation map on the input MRI image, which highlights the tumor region. Figure 7 shows the segmenting result of a tumor region, and Figure 8 shows that of a non-tumor region. Combining these two models will bring huge value for doctors' clinical diagnosis and effective treatment planning.

“Focal Tversky Loss and Focal Tversky Accuracy” are modified evaluation metrics from the standard “Tversky Loss and Accuracy functions”, respectively. They were introduced in the paper by Abraham et al., titled "Focal Tversky loss function with improved Attention U-Net for lesion segmentation" [40]. It has stronger penalties for “false positives and false negatives” compared to its vanilla version and hence can give more accurate detection when classes are small and infrequent. It is a hyperparameter of this metric that is responsible for the balance between false positives and negatives and positively influences the sensitivity of the model, as presented in Figure 9.

The “Focal Tversky Accuracy” metric is a modification of the regular Tversky Accuracy, with targeting for small and rare classes. It takes the same “focusing parameter γ as in Focal Tversky Loss”,

which helps balance the weight between "false positives and false negatives", therefore making this metric more effective for scenarios where rare or small tumor regions need to be detected. Refer to Figure 9.

In general, these modified evaluation metrics have been proven to improve the segmentations of the models in various image segmentation tasks, including Brain Tumor Segmentation, especially where sensitivity and accuracy are critical factors.

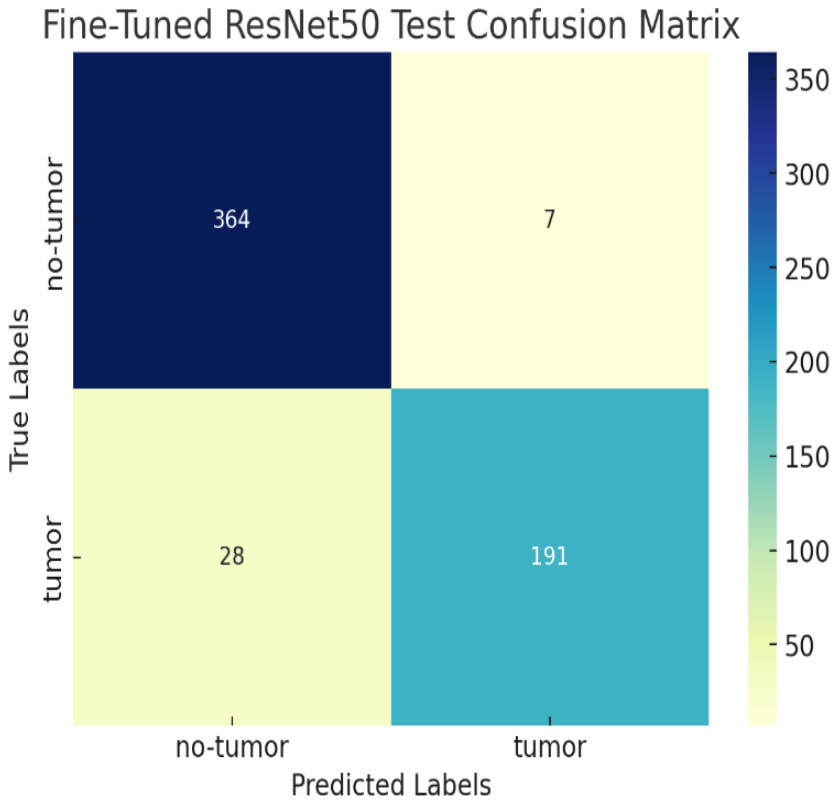

Figure 5. Confusion matrix for fine-tuned ResNet50 model.

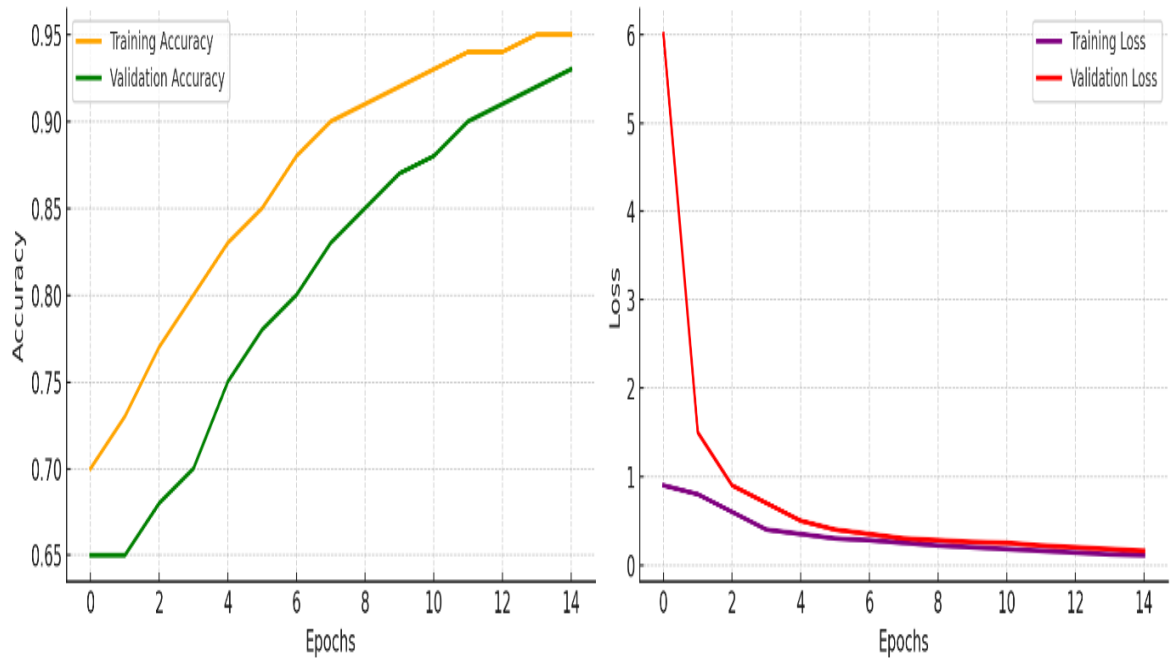

Figure 6. Accuracy and loss graph.

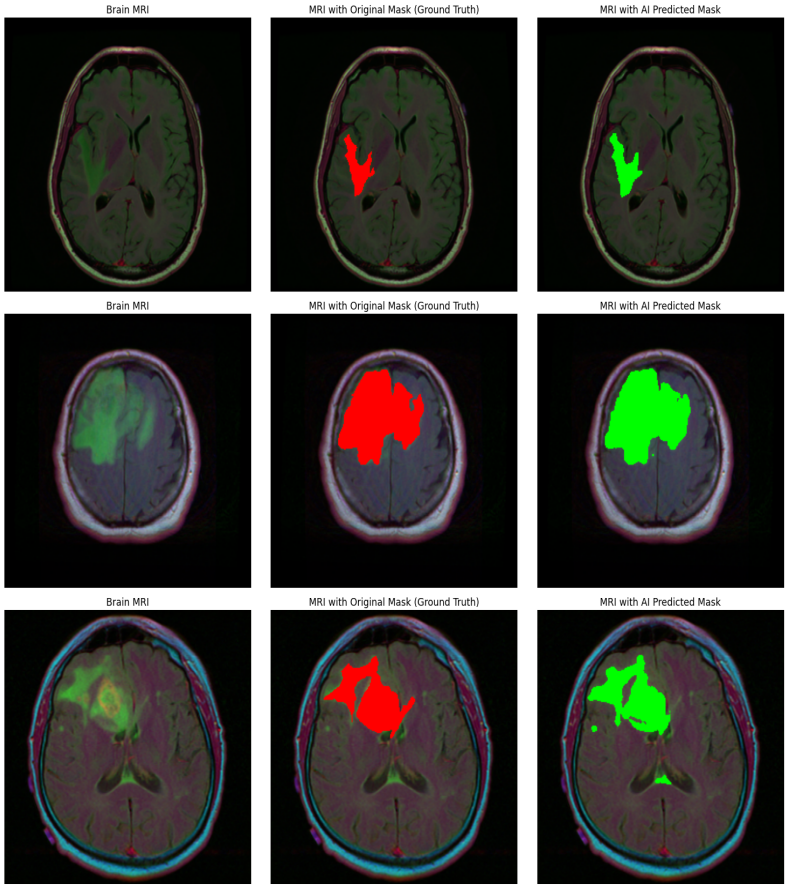

Figure 7. Model prediction of tumor regions.

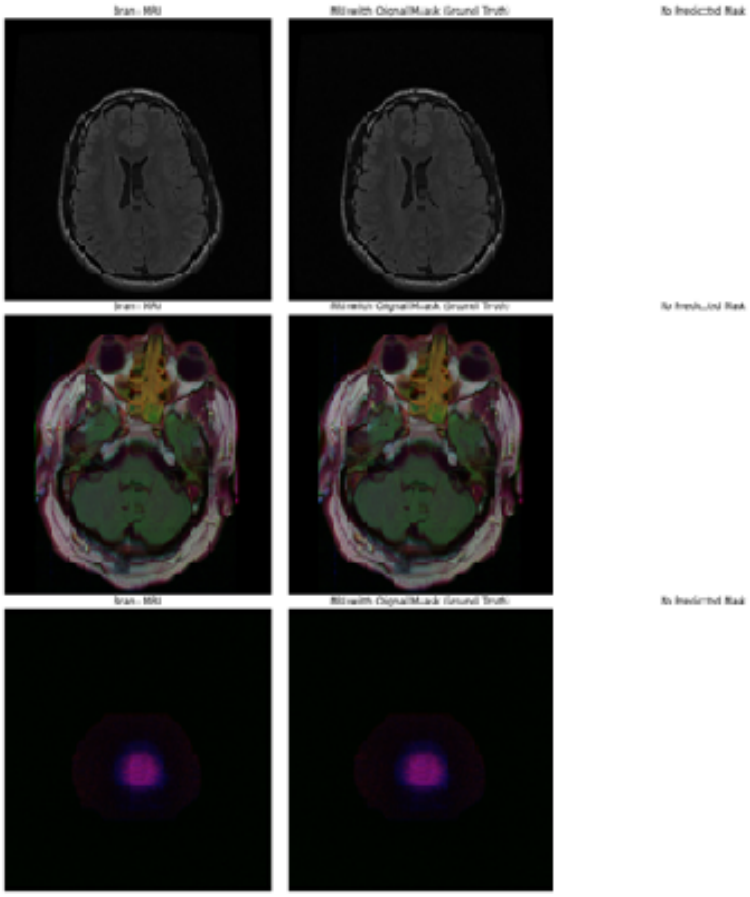

Figure 8. Model prediction of no-tumor regions.

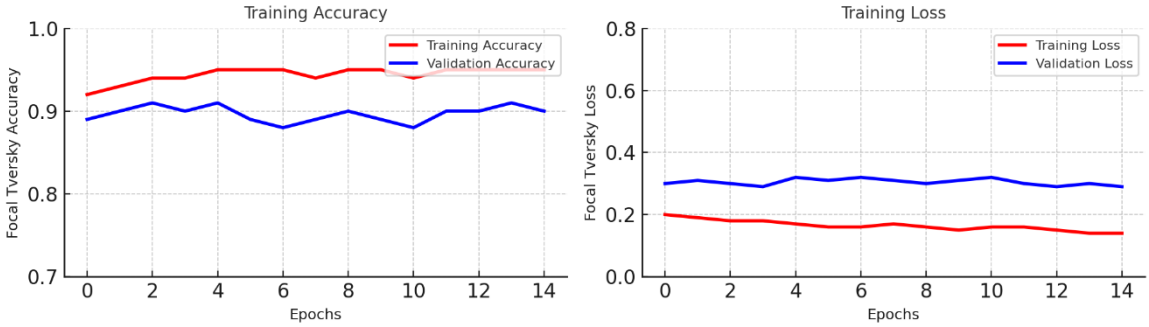

Figure 9. Focal Tversky Accuracy and Loss.

5. Evaluation Metrics

The segmentation and classification evaluation process includes many of the following evaluation criteria. Below are a few equations used for evaluation:

- True Positive (TP): A real positive outcome is when the model is able to accurately predict the 'positive class' label.
- False Positive (FP): Assume that the estimated value is positive, and the actual value is negative.
- True Negative (TP): An accurate negative is an outcome in which the model rightly predicts the negative category.
- False Negative (FN): False Negatives (FN) represent negative results that the model misunderstood in its prediction.
- Accuracy: Accuracy measures how accurately the model predicts the outcome. The proportion of real samples in the dataset is shown in Equation (5).

$$Accuracy = \frac{TP+TN}{TP+FP+TN+FN} \quad (5)$$

- Precision: The ratio of those identified as positive to all positive samples as shown in Equation (6).

$$Precision = \frac{TP}{TP+FP} \quad (6)$$

- Recall: The ratio of the correctly identified quality to the total quality of the sample is shown in Equation (7).

$$Recall = \frac{TP}{TP+FN} \quad (7)$$

- F1 Score: The harmonic means of precision and recall contribute to equal weighting for both parameters, as shown in Equation (8).

$$F1 - score = \frac{2 \times (Precision \times Recall)}{Precision+Recall} \quad (8)$$

- Dice Similarity Coefficient: Compare dice coefficient with IOU. Because they are closely related, if one person says model A is better at image segmentation than model B, others will say the same. They vary between 0 and 1; where 1 is the similarity between prediction and reality, similar to IOU. Statistical accuracy measures the performance of most electronic components of MR images and the reliability of manual segmentation and layering accuracy.

$$DSC = \frac{TP}{\frac{1}{2}(2TP+FP+FN)} \quad (9)$$

- Intersection over Union (IOU): Intersection over Union (IOU) serves as an evaluation metric for algorithms related to annotation, segmentation, and object detection. The analysis of the similarity between the actual bounding box or annotated region and the predicted bounding box or segmented area comes from it.

$$IOU = \frac{TP}{TP+FP+FN} \quad (10)$$

- Similarity index (SI): SI is important for accurate assessment of tumor size. It measures the similarity between the actual description and the segmented object. Higher SI values indicate diagnostic accuracy as well as better agreement between predicted segmentation and real cases. These tests help evaluate the function and classification patterns of tumor cells by measuring their ability to identify positive and negative patterns. To evaluate the effectiveness of these models and check them against other methods.

$$SI = \frac{2TP}{2TP+FP+FN} \quad (11)$$

A fine-tuning combined method of ResNet50 and U-Net with the convolutional neural network model perhaps works powerfully in comprehensive brain tumor detection, classification, and segmentation. Maximum advantage has been taken from the capabilities of each model in order to enhance the overall accuracy.

6. Discussion

Accordingly, U-Net integrated with ResNet50 was able to achieve a "Dice Coefficient of 0.95, IOU of 0.91, and SI of 0.95", as reflected in Table 3 below. Further, this study compares two models, "CNN and fine-tuned ResNet50", for the classification performance of brain tumors from MRI images as shown in Table 2. The result indeed proves that the fine-tuned ResNet50 outperforms the CNN by a significant margin on both non-tumor and tumor classes with respect to "precision, recall, F1 score, and accuracy". In the case of fine-tuned ResNet50, the class "non-tumor" attained a "precision of 0.98, recall of 0.95, F1 score of 0.93, and accuracy of 0.94", proving that it was able to classify correctly a good percentage of cases under complete negative conditions.

Table 3. The following is the statistical values of the model which has U-Net architecture with fine-tuned Resnet50.

Reference	Segmentation Techniques	Dataset	Results
[41]	Multi-level threshold technique	BRATS 2015	DSC 0.89
[42]	K-means	BRATS 2017	SI 0.91
[43]	Random	BRATS 2012	DSC 0.91
[44]	Darwinian Particle Swarm Optimization	BRATS 2015	DSC 0.93
[45]	Morphological Technique	BRATS 2015	DSC 0.90
Our method	ResUNet with fine-tuned Resnet50	TCGA-LGG and TCIA	SI 0.95, IOU 0.91, DSC 0.95

For the tumor class, the ResNet50 model has a "precision of 0.87, a recall of 0.92, an F1 score of 0.88, and the accuracy is 0.96", where the number of correctly classified cases for the tumor class is good. These results justify that the fine-tuned ResNet50 model has a better detection ability of the brain tumor from MRI images; therefore, the treatment may result in more effective and personalized treatments best fitted to the particular needs of each patient. These quantified performance metrics of the "model-IOU: 0.91, DSC: 0.95, and SI: 0.95" have critical implications for medical image analysis and have the potential of further enhancing patient outcomes.

Therefore, one of the main limitations of the study is the fact that it was based on freely available datasets. "TCGA-LGG and TCIA" may not include all the scenarios faced in cases of brain tumors and thus are susceptible to biases. The performance metrics identified in this study may not fully represent the real clinical perspective, and further validation is required on much larger datasets with diversity.

7. Conclusions

This study proposes a CNN that incorporates fine-tuned ResNet50 with U-Net architecture for brain tumor classification and detection in MRI images. The fine-tuning of ResNet50 has been utilized for tumor detection, while the U-Net architecture is used for segmentation, delineating the tumor from surrounding healthy tissue with high accuracy. It comes out with a pre-trained ResNet50 that outperforms the simple CNN by the performance measures, as it has "precision 0.98, recall 0.95, F1 score 0.93, and accuracy 0.94 for the non-tumor class, while for the tumor class, the respective values are "0.87, 0.92, 0.88, and 0.96".

From the segmentation result of this model, "IOU is 0.91, DSC is 0.95, and SI is 0.95". These results confirm that fine-tuning ResNet50 is very effective for the detection and classification of brain tumors with high accuracy, making it an important tool for enhancing clinical diagnosis and treatment conclusions.

Data Availability Statement: Dataset is publicly available and can be downloaded from the given link: https://wiki.cancerimagingarchive.net/pages/viewpage.action?pageId=5309188

References

1. Muhammad Abdullah Aish, Amina Abdul Ghafoor, Fawad Nasim, Kiran Irfan Ali, Shamim Akhter, & Sumbul Azeem. (2024). Improving Stroke Prediction Accuracy through Machine Learning and Synthetic Minority Over-sampling. Journal of Computing & Biomedical Informatics, 7(02). Retrieved from https://jcbi.org/index.php/Main/article/view/566
2. Asiri, A.A.; Aamir, M.; Shaf, A.; Ali, T.; Zeeshan, M.; Irfan, M.; Alshamrani, K.A.; Alshamrani, H.A.; Alqahtani, F.F.; Alshehri, A.H.D. Block-Wise Neural Network for Brain Tumor Identification in Magnetic Resonance Images. Comput. Mater. Contin. 2022, 73, 5735–5753. https://doi.org/10.32604/cmc.2022.031747
3. Asiri, A.A.; Shaf, A.; Ali, T.; Aamir, M.; Usman, A.; Irfan, M.; Alshamrani, H.A.; Mehdar, K.M.; Alshehri, O.M.; Alqhtani, S.M. Multi-Level Deep Generative Adversarial Networks for Brain Tumor Classification on Magnetic Resonance Images. Intell. Autom. Soft Comput. 2023, 36, 127–143. https://doi.org/10.32604/iasc.2023.032391
4. Siegel, R.L.; Miller, K.D.; Jemal, A. Cancer statistics, 2015. CA Cancer J. Clin. 2015, 65, 5–29. https://doi.org/10.3322/caac.21254
5. Goding Sauer, A.; Siegel, R.L.; Jemal, A.; Fedewa, S.A. Current prevalence of major cancer risk factors and screening test use in the United States: Disparities by education and race/ethnicity. Cancer Epidemiol. Prev. Biomark. 2019, 28, 629–642. https://doi.org/10.1158/1055-9965.EPI-18-1169
6. Ostrom, Q.T.; Gittleman, H.; Truitt, G.; Boscia, A.; Kruchko, C.; Barnholtz-Sloan, J.S. CBTRUS Statistical report: Primary brain and other central nervous system tumors diagnosed in the United States in 2011–2015. Neuro. Oncol. 2018, 20 (Suppl. S4), iv1–iv86. https://doi.org/10.1093/neuonc/noy131
7. Abiwinanda, N.; Hanif, M.; Hesaputra, S.T.; Handayani, A.; Mengko, T.R. Brain tumor classification using convolutional neural network. In Proceedings of the World Congress on Medical Physics and Biomedical Engineering 2018, Prague, Czech Republic, 3–8 June 2018; Springer: Singapore, 2019.
8. Abir, T.A.; Siraji, J.A.; Ahmed, E.; Khulna, B. Analysis of a novel MRI based brain tumour classification using probabilistic neural network (PNN). Int. J. Sci. Res. Sci. Eng. Technol. 2018, 4, 65–79.
9. Naseer, A.; Rani, M.; Naz, S.; Razzak, M.I.; Imran, M.; Xu, G. Refining Parkinson's neurological disorder identification through deep transfer learning. Neural Comput. Appl. 2020, 32, 839–854. https://doi.org/10.1007/s00521-019-04069-0
10. Núñez-Martín, R.; Cervera, R.C.; Pulla, M.P. Gastrointestinal stromal tumour and second tumours: A literature review. Med. Clínica 2017, 149, 345–350. (In English) https://doi.org/10.1007/s00521-019-04069-0
11. Kleesiek, J.; Biller, A.; Urban, G.; Köthe, U.; Bendzsus, M.; Hamprecht, F.A. Ilastik for multi-modal brain tumor segmentation. In Proceedings of the MICCAI BraTS (Brain Tumor Segmentation Challenge), Boston, MA, USA, 14 September 2014; pp. 12–17.
12. Meier, R.; Bauer, S.; Slotboom, J.; Wiest, R.; Reyes, M. Appearance-and context-sensitive features for brain tumor segmentation. In Proceedings of the MICCAI BraTS Challenge, Boston, MA, USA, 14 September 2014; pp. 20–26.
13. Long, J.; Shelhamer, E.; Darrell, T. Fully convolutional networks for semantic segmentation. In Proceedings of the IEEE Conference on Computer Vision and Pattern Recognition, Boston, MA, USA, 7–12 June 2015.
14. Rehman, A.; Naz, S.; Razzak, M.I.; Hameed, I.A. Automatic visual features for writer identification: A deep learning approach. IEEE Access 2019, 7, 17149–17157. https://doi.org/10.1109/ACCESS.2018.2890810
15. Cheng, J. Brain Tumor Dataset. Figshare. Dataset. 2017. Available online: https://figshare.com/articles/braintumordataset/1512427.
16. von Baumgarten, L.; Brucker, D.; Tirniceru, A.; Kienast, Y.; Grau, S.; Burgold, S.; Herms, J.; Winkler, F. Bevacizumab has differential and dose-dependent effects on glioma blood vessels and tumor cells. Clin. Cancer Res. 2011, 17, 6192–6205. https://doi.org/10.1158/1078-0432.CCR-10-1868
17. Ferluga, S.; Baiz, D.; Hilton, D.A.; Adams, C.; Ercolano, E.; Dunn, J.; Bassiri, K.; Kurian, K.M.; Hanemann, C.O. Constitutive activation of the EGFR–STAT1 axis increases proliferation of meningioma tumor cells. Neuro-Oncol. Adv. 2020, 2, vdaa008. https://doi.org/10.1093/noajnl/vdaa008
18. Satou, M.; Wang, J.; Nakano-Tateno, T.; Teramachi, M.; Suzuki, T.; Hayashi, K.; Lamothe, S.; Hao, Y.; Kurata, H.; Sugimoto, H.; et al. L-type amino acid transporter 1, LAT1, in growth hormone-producing pituitary tumor cells. Mol. Cell. Endocrinol. 2020, 515, 110868. https://doi.org/10.1016/j.mce.2020.110868
19. Sharif Razavian, A.; Azizpour, H.; Sullivan, J.; Carlsson, S. CNN features off-the-shelf: An astounding baseline for recognition. In Proceedings of the IEEE Conference on Computer Vision and Pattern Recognition Workshops, Columbus, OH, USA, 23–28 June 2014.

20. Deng, J.; Dong, W.; Socher, R.; Li, L.J.; Li, K.; Fei-Fei, L. Imagenet: A large-scale hierarchical image database. In Proceedings of the 2009 IEEE Conference on Computer Vision and Pattern Recognition, Miami, FL, USA, 20–25 June 2009; IEEE: Piscataway, NJ, USA, 2009.
21. Everingham, M.; Eslami, S.M.A.; Van Gool, L.; Williams, C.K.I.; Winn, J.; Zisserman, A. The pascal visual object classes challenge: A retrospective. Int. J. Comput. Vis. 2015, 111, 98–136. https://doi.org/10.1007/s11263-014-0733-5
22. Cheng, J.; Huang, W.; Cao, S.; Yang, R.; Yang, W.; Yun, Z.; Wang, Z.; Feng, Q. Enhanced performance of brain tumor classification via tumor region augmentation and partition. PLoS ONE 2015, 10, e0140381. https://doi.org/10.1371/journal.pone.0140381
23. Ismael, M.R.; Abdel-Qader, I. Brain tumor classification via statistical features and backpropagation neural network. In Proceedings of the 2018 IEEE International Conference on Electro/Information Technology (EIT), Rochester, MI, USA, 3–5 May 2018; IEEE: Piscataway, NJ, USA, 2018.
24. Shakeel, P.M.; Tobely, T.E.E.; Al-Feel, H.; Manogaran, G.; Baskar, S. Neural network based brain tumor detection using wireless infrared imaging sensor. IEEE Access 2019, 7, 5577–5588. https://doi.org/10.1109/ACCESS.2018.2883957
25. Setio, A.A.; Ciompi, F.; Litjens, G.; Gerke, P.; Jacobs, C.; van Riel, S.J.; Wille, M.M.; Naqibullah, M.; Sanchez, C.I.; van Ginneken, B. Pulmonary nodule detection in CT images: False positive reduction using multi-view convolutional networks. IEEE Trans. Med. Imaging 2016, 35, 1160–1169. https://doi.org/10.1109/TMI.2016.2536809
26. Al-Ayyoub, M.; Husari, G.; Darwish, O.; Alabed-alaziz, A. Machine learning approach for brain tumor detection. In Proceedings of the 3rd International Conference on Information and Communication Systems, Irbid, Jordan, 3–5 April 2012.
27. Parihar, A.S. A study on brain tumor segmentation using convolution neural network. In Proceedings of the 2017 International Conference on Inventive Computing and Informatics (ICICI), Coimbatore, India, 23–24 November 2017; IEEE: Piscataway, NJ, USA, 2017.
28. Sultan, H.H.; Salem, N.M.; Al-Atabany, W. Multi-classification of brain tumor images using deep neural network. IEEE Access 2019, 7, 69215–69225. https://doi.org/10.1109/ACCESS.2019.2919122
29. Ismael, S.A.A.; Mohammed, A.; Hefny, H. An enhanced deep learning approach for brain cancer MRI images classification using residual networks. Artif. Intell. Med. 2020, 102, 101779. https://doi.org/10.1016/j.artmed.2019.101779
30. Abdalla, H.E.M.; Esmail, M. Brain tumor detection by using artificial neural network. In Proceedings of the 2018 International Conference on Computer, Control, Electrical, and Electronics Engineering (ICCCEEE), Khartoum, Sudan, 12–14 August 2018; IEEE: Piscataway, NJ, USA, 2018.
31. Vinoth, R.; Venkatesh, C. Segmentation and Detection of Tumor in MRI images Using CNN and SVM Classification. In Proceedings of the 2018 Conference on Emerging Devices and Smart Systems (ICEDSS), Tiruchengode, India, 2–3 March 2018; IEEE: Piscataway, NJ, USA, 2018.
32. Rehman, A.; Naz, S.; Razzak, M.I.; Akram, F.; Imran, M. A deep learning-based framework for automatic brain tumors classification using transfer learning. Circuits Syst. Signal Process. 2020, 39, 757–775. https://doi.org/10.1007/s00034-019-01246-3
33. Swati, Z.N.K.; Zhao, Q.; Kabir, M.; Ali, F.; Ali, Z.; Ahmed, S.; Lu, J. Brain tumor classification for MR images using transfer learning and fine-tuning. Comput. Med. Imaging Graph. 2019, 75, 34–46. https://doi.org/10.1016/j.compmedimag.2019.05.001
34. Ahmed, K.B.; Hall, L.O.; Goldgof, D.B.; Liu, R.; Gatenby, R.A. Fine-tuning convolutional deep features for MRI based brain tumor classification. In Proceedings of the Medical Imaging 2017: Computer-Aided Diagnosis, Orlando, FL, USA, 3 March 2017; SPIE: Bellingham, WA, USA, 2017.
35. Pedano, N.; Flanders, A.E.; Scarpace, L.; Mikkelsen, T.; Eschbacher, J.M.; Hermes, B.; Sisneros, V.; Barnholtz-Sloan, J.; Ostrom, Q. Radiology Data from The Cancer Genome Atlas Low Grade Glioma [TCGA-LGG] collection. Cancer Imaging Arch. 2016.
36. Khan, M. F., Iftikhar, A., Anwar, H., & Ramay, S. A. (2024). Brain Tumor Segmentation and Classification using Optimized Deep Learning. Journal of Computing & Biomedical Informatics, 7(01), 632-640.
37. Clark, K.; Vendt, B.; Smith, K.; Freymann, J.; Kirby, J.; Koppel, P.; Moore, S.; Phillips, S.; Maffitt, D.; Pringle, M.; et al. The Cancer Imaging Archive (TCIA): Maintaining and operating a public information repository. J. Digit. Imaging 2013, 26, 1045–1057. https://doi.org/10.1007/s10278-013-9622-7

38. Aamir, M.; Irfan, M.; Ali, T.; Ali, G.; Shaf, A.; Al-Beshri, A.; Alasbali, T.; Mahnashi, M.H. An adoptive threshold-based multi-level deep convolutional neural network for glaucoma eye disease detection and classification. Diagnostics 2020, 10, 602. https://doi.org/10.3390/diagnostics10080602
39. Aamir, M.; Ali, T.; Shaf, A.; Irfan, M.; Saleem, M.Q. ML-DCNNet: Multi-level deep convolutional neural network for facial expression recognition and intensity estimation. Arab. J. Sci. Eng. 2020, 45, 10605–10620. https://doi.org/10.1007/s13369-020-04811-0
40. Jie, H.J.; Wanda, P. RunPool: A dynamic pooling layer for convolution neural network. Int. J. Comput. Intell. Syst. 2020, 13, 66–76. https://doi.org/10.2991/ijcis.d.200120.002
41. Khan, M. F., Iftikhar, A., Anwar, H., & Ramay, S. A. (2024). Brain Tumor Segmentation and Classification using Optimized Deep Learning. Journal of Computing & Biomedical Informatics, 7(01), 632-640.
42. Abraham, N.; Khan, N.M. A novel focal tversky loss function with improved attention u-net for lesion segmentation. In Proceedings of the 2019 IEEE 16th International Symposium on Biomedical Imaging (ISBI 2019), Venice, Italy, 8–11 April 2019; IEEE: Piscataway, NJ, USA, 2019.
43. Rajinikanth, V.; Fernandes, S.L.; Bhushan, B.; Harisha; Sunder, N.R. Segmentation and analysis of brain tumor using Tsallis entropy and regularised level set. In Proceedings of 2nd International Conference on Micro-Electronics, Electromagnetics and Telecommunications: ICMEET 2016; Springer: Singapore, 2018.
44. Bal, A.; Banerjee, M.; Sharma, P.; Maitra, M. Brain tumor segmentation on MR image using K-Means and fuzzy-possibilistic clustering. In Proceedings of the 2018 2nd International Conference on Electronics, Materials Engineering & Nano-Technology (IEMENTech), Kolkata, India, 4–5 May 2018; IEEE: Piscataway, NJ, USA, 2018.
45. Shanker, R.; Singh, R.; Bhattacharya, M. Segmentation of tumor and edema based on K-mean clustering and hierarchical centroid shape descriptor. In Proceedings of the 2017 IEEE International Conference on Bioinformatics and Biomedicine (BIBM), Kansas City, MO, USA, 13–6 November 2017; IEEE: Piscataway, NJ, USA, 2017.
46. Mehidi, I.; Belkhiat, D.E.C.; Jabri, D. An improved clustering method based on K-means algorithm for MRI brain tumor segmentation. In Proceedings of the 2019 6th International Conference on Image and Signal Processing and their Applications (ISPA), Mostaganem, Algeria, 24–25 November 2019; IEEE: Piscataway, NJ, USA, 2019.
47. Rundo, L.; Militello, C.; Russo, G.; Vitabile, S.; Gilardi, M.C.; Mauri, G. GTV cut for neuro-radiosurgery treatment planning: An MRI brain cancer seeded image segmentation method based on a cellular automata model. Nat. Comput. 2018, 17, 521–536. https://doi.org/10.1007/s11047-017-9636-z